Int. J. Nano Dimens., 10 (3): 242-251, Summer 2019

ORIGINAL ARTICLE

Study on structural, luminescence properties and Hall Effect of SnO_2 nanoparticles obtained by a Co-precipitation technique

Suresh Gopal[1], Sathishkumar Rajagemberam[1], Baskaran Iruson[1,*], Sathyaseelan Balaraman[2], Senthilnathan Krishnmoorthy[3], Manikandan Elayaperumal[4]

[1] Department of Physics, Arignar Anna Govt. Arts College, Cheyyar-604407, Tamil Nadu, India.

[2] Department of Physics, University College of Engineering Arni , Anna University Chennai, Arni 632326, Tamil Nadu, India.

[3] Department of Physics, VIT University, Vellore-632014, Tamilnadu, India.

[4] Department of Physics, Thiruvalluvar University, TVUCAS Campus, Thennangur, 604408, Tamil Nadu, India.

Received 12 November 2018, revised 03 January 2019, accepted 04 February 2019, available online 07 February 2019

Abstract

In this paper, we report the synthesis of tin oxide (SnO_2) nanoparticles by co-precipitation technique. The structural, surface morphology, thermal and optical properties of the SnO_2 samples were analysed using X-ray diffraction (XRD), High-resolution transmission electron microscopy (HRTEM), Fourier transformed infrared (FTIR) spectrum, thermo gravimetric analysis (TGA/DTA), photoluminescence spectrum (PL) and UV–Vis spectroscopy techniques. X-ray diffraction patterns showed the SnO_2 crystallites with the tetragonal rutile structure and UV-Vis analysis showed the characteristic absorbance peak at 345 nm. In the PL emission spectrum, three peaks were found at 500, 605 and 651nm, due to the oxygen vacancy defect. Finally, Hall coefficient was also estimated for various values of an applied magnetic field and bias current applied to the SnO_2 sample. From the detailed study, it has been found that the prepared sample is an n-type semiconductor.

Keywords: *Hall Effect; Luminescence; Nanoparticles; Semiconducting materials; Tin Oxide.*

How to cite this article

Gopal S, Rajagemberam S, Iruson B, Balaraman S, Krishnmoorthy S, Elayaperumal M. Study on structural, luminescence properties and Hall Effect of SnO_2 nanoparticles obtained by a Co-precipitation technique. Int. J. Nano Dimens., 2019; 10 (3): 242-251.

INTRODUCTION

The words nanoscience and nanotechnology have become most common in day to day life. In recent years, Nanomaterials have gained a huge momentum as they exhibit unusual intriguing properties as well as enhanced properties when compared to bulk materials. The semiconductor nanocrystals are of significant interest and focus in the last decades owing to their technological applications. The electrical, optical and magnetic properties of such particles are highly dependent on the size of the particle [1]. It is established that SnO_2 is an n-type semiconductor which has a wide band gap, Eg, of 3.64 eV. The valence band is closed shell of oxygen $2S^2$, $2P^6$ state mixed with some Sn states. The structure of the material in its bulk form is tetragonal rutile [2]. The sign of the Hall voltage determines the type of the carriers (+ for p-type, - for n-type) semiconductor. Sn forms an interstitial bond with oxygen and exists either as SnO or SnO_2, hence has a valency of +2 or +4, respectively. This valency state has a direct bearing on the ultimate conductivity of Tin Oxide. The lower valence state results in a net reduction in carrier concentration since a hole is created which acts as a trap and reduces conductivity. On the other hand, predominance of SnO_2 state means Sn^{4+} acts as an n-type donor-releasing electron to the conduction band. The large value of n indicates that Sn forms bond with oxygen and exists as SnO_2. It is found that the SnO_2 behave as n-type semi-conductors. It finds a wide range of applications such as transparent conducting electrodes, solid-state gas sensors [3], devices in

* Corresponding Author Email: *ibk1978@gmail.com*

liquid crystal display, rechargeable Li batteries [4] photoconductive, gas discharge display, catalyst [5], spintronics, optoelectronics devices, etc. [6].

So far, several techniques for synthesizing SnO_2 nanostructures have been proposed, namely, spray pyrolysis, hydrothermal, methods, chemical vapour deposition, thermal evaporations of tin oxide powder and sol-gel [7] and co-precipitation method. Of these methods, in this work, we choose the co-precipitation method for synthesizing SnO_2 nanostructured materials because of its relatively low processing cost, much milder and the ability to control the grain size [8]. After the successful preparation of the material, the important characteristics, namely, structural analysis, optical and thermal properties have been studied.

EXPERIMENT

The SnO_2 nanocrystalline materials were prepared by the chemical co-precipitation method. All the chemical reagents were used of AR grade. Tin(IV) chloride pent hydrate $SnCl_4.5H_2O$ 98% [Chemicals, India] and ammonia solution $NH_3.H_2O$ 30% [Loba Chemicals, India] were used as starting materials. The co-precipitation technique was used for the synthesis of tin oxide nanopowder. In the synthesis process (Flowchart Fig. 1), Tin (IV) chloride pent hydrate (3.5058 gram of $SnCl_4.5H_2O$) was dissolved in 100 mL double distilled water in a beaker and 100mL of ethanol was added into the beaker. The resulting precursor mixture was kept for stirring on a magnetic stirrer (make: Remi) at 3000 rpm for 30 minutes. Further, 4 mL an aqueous ammonia solution was added to this solution by stirring this mixture with a rate of 10 drops/ minute. During this process, the dropping rate was well controlled for the chemical homogeneity to from white slurry. The resulting slurry was filtered by using pore size of whatman filter paper no 42 and then washed for 3 hours with double distilled water to remove the impurities by washing 4 times. The resulting precipitate was heated in an oven at 50 °C for 8 hours to remove water molecules and calcinated at 230 °C for 2 hours

The prepared sample was characterized by a Philips PW1700 (operated at 40 kV and current of 30 mA) XRD to study the crystalline phase structure. Here, the sample was scanned between 200 and 800 at a scanning speed of 0.020/sec with Cu Kα (λ=1.5406 ◦A) as a radiation source. The FTIR spectrum of the sample was studied using an AVATAR 360 spectrometer with KBr as

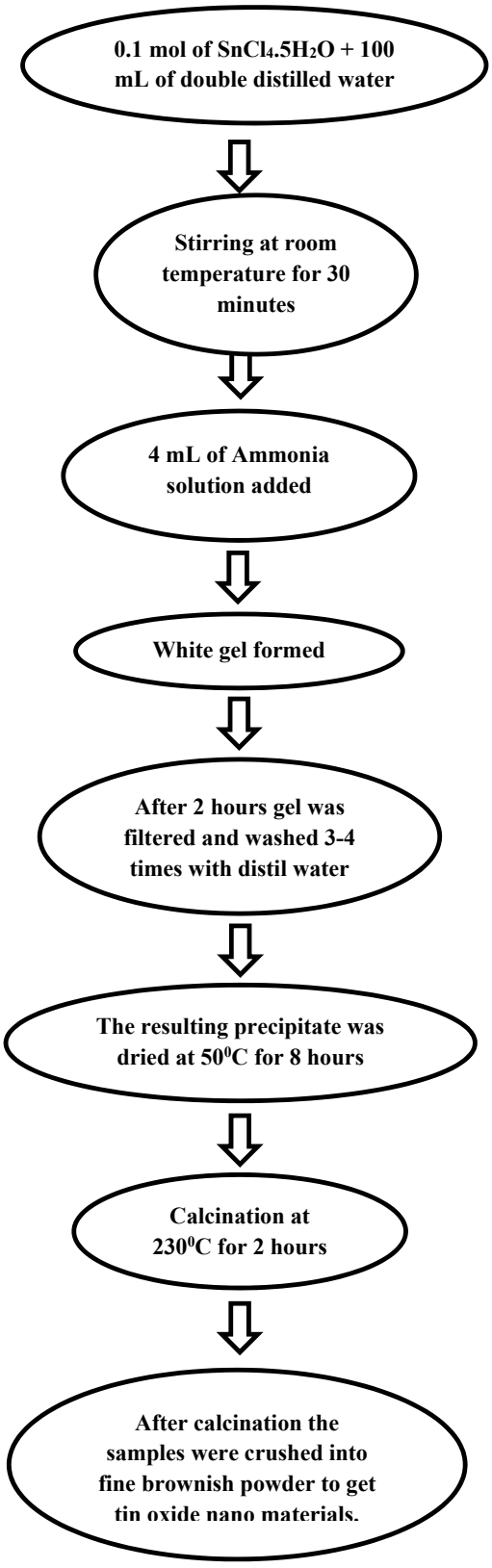

Fig. 1. Flow chart of synthesis of SnO_2.

compressed slices in the range of 4000-400 cm^{-1}. An optical absorption spectrum of the sample was recorded with OPTIMA SP-3000 UV-VIS spectrometer. The PL measurements were carried out at room temperature using 275 nm as the excitation wavelength with a Hitachi f-4500 FL Spectrophotometer where Xe lamp is used as the excitation source. In addition, HRTEM was taken with a JEOL – 3010 operating at 200 KV. The thermal behaviour of as dried sample was investigated by shimadzu DTA-60H apparatus.

RESULTS AND DISCUSSION

Structural properties by XRD

The XRD is used to identify the crystalline structure and average particle size of the samples. XRD pattern of the prepared SnO_2 is shown in Fig. 1. The diffraction peaks have been indexed to the tetragonal rutile phase of SnO2 JCPDS Card No.88-0287, a=4.737 ◦A, c=3.186 ◦A [1]. It is to be noted that no other crystalline by-products are found in the pattern which indicates that the as-prepared sample has a pure rutile structure with good crystallinity. From Fig. 2, it is clear that the relative intensities of (110) peak are the largest [9]. In Table 1, the experimental data have been compared with JCPDS data. Having the explored the structural analysis, the next step is to calculate the average size of the particle. Here, the average particle size was calculated using the Scherrer's formula.

$$D = K\lambda / \beta\cos\theta$$

where D is the average crystallite size, K is the shape factor usually has a value 0.9, λ is the X-Ray wavelength and θ is the Bragg diffraction angle of the diffraction peaks and β gives the full width of the half maxima (FWHM). By using the above formula, the average particle size was found to be 24 nm.

Thermal behaviour of SnO_2 nanoparticles

The thermal analysis of SnO_2 using TG-DTA/ DSC is shown in Fig. 3. The weight loss is due to the elimination of ammonia, physically adsorbed water, and chemically bonded water. Hence, the total weight loss is 17.13%, which occurred in two stages: I and II. A large amount of weight loss (12.92%) appears in the first stage in the

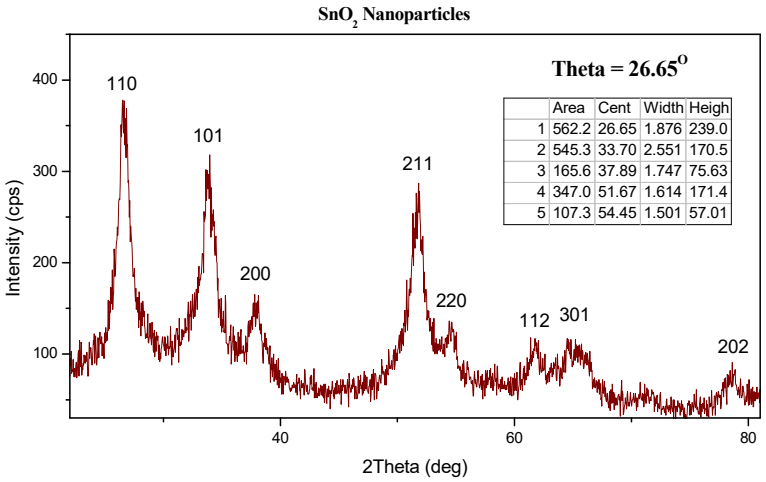

Fig. 2. XRD pattern of SnO_2 nanocrystalline.

Table 1. XRD analysis of SnO_2 Nanocrystalline.

2 theta (degree)	(hkl) planes	Inter-planar distances (d) in nm
26.65	(110)	58.9
33.70	(101)	55.3
51.67	(200)	43.6
54.45	(211)	59.7
61.81	(220)	57.7
64.87	(310)	49.3
78.40	(301)	51.7

temperature range between room temperature and 145.8◦C which is attributed to dehydration of water molecules on the surface of particles. This process was confirmed by an exothermic peak at 107.1°C, -0.1665 mW / mg around the area of 36.3 J/gin DSC. In the second stage, melting takes place from 145.1°C to 560°C that corresponds to the elimination of the hydroxyl group and decomposition of ammonia, respectively. This process was described by an Endothermic peak around at 441 °C, -1.78 mW / mg around area 56.82 J/g in DSC [10, 12]. The weight loss in this stage is 6.91%. After 560 °C, the weight loss was occurred due to the elimination of the little amount of residual hydroxyl group during the development of tin dioxide nanoparticles. The peak around 1299.3°C is corresponding to maybe decomposition or sublimation of NH_3 [10-11].

Fourier transforms spectroscopy (FTIR)

It is well known that FTIR is usually employed as an additional probe to identify the presence of O-H group as well as other organic& inorganic species. The FTIR spectrum in the range 4000-400

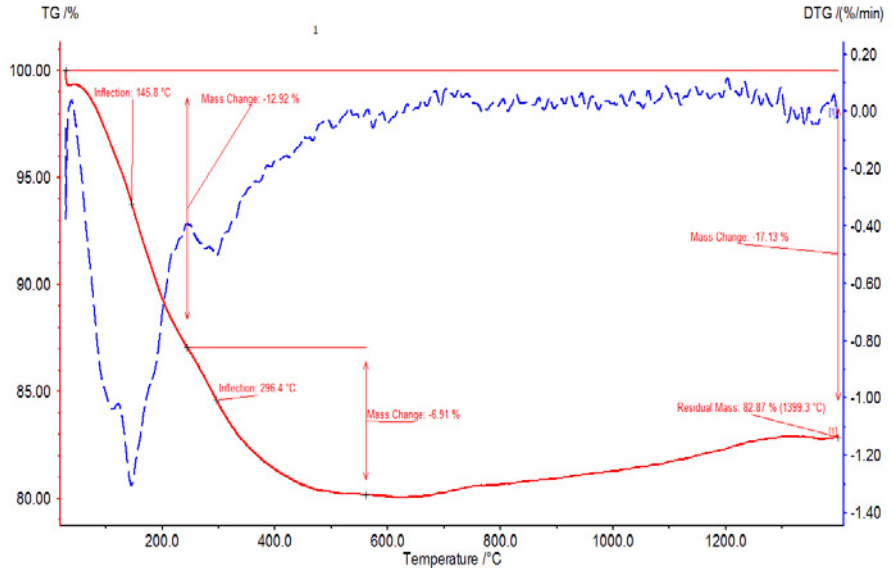

Fig. 3. TGA and DSC curves for dried sample.

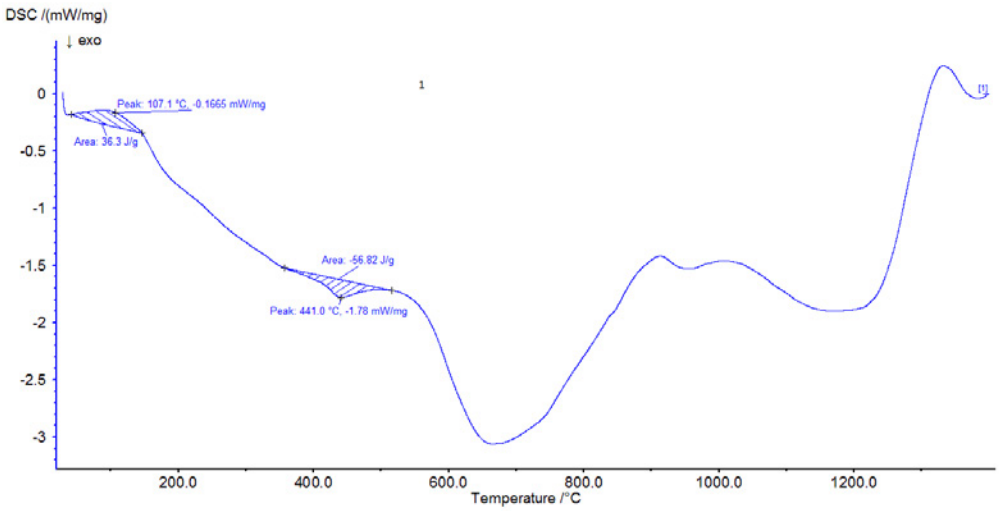

Fig. 4. DSC curves for dried sample.

cm^{-1} of the as-synthesized sample is depicted in Fig. 4. For the as-synthesized SnO_2 nanostructures, the spectra were recorded in the range of 400–4000 cm^{-1} for confirmation of SnO_2. The band appears in the value of 1020.3 cm^{-1} is assigned to Sn–O antisymmetric vibration for all the samples. The peaks in the range of 1634.26 cm^{-1} and 3397–3872 cm^{-1} are related to the OH stretching of the hydroxyl group. There is no band observed for the existence of CO_2 molecule in the air. The broadband 619 cm^{-1} is attributed to the framework vibrations of the O-Sn-O bond in SnO_2 [6].

Optical Properties

The absorption spectrum of the SnO_2 nanoparticle is shown in Figs. 5 and 6, and the value of the absorption is 344.99(8) nm. Considering the blue of the absorption positions from the bulk SnO_2, the absorption onsets of the present samples can be assigned to the direct transition of an electron in the SnO_2 nanocrystals. The optical band gap energy (Eg) of the corresponding samples is calculated by Tauc plot by using the following equation,

$\alpha(h\nu) = A\ (h\nu - Eg)^n$,

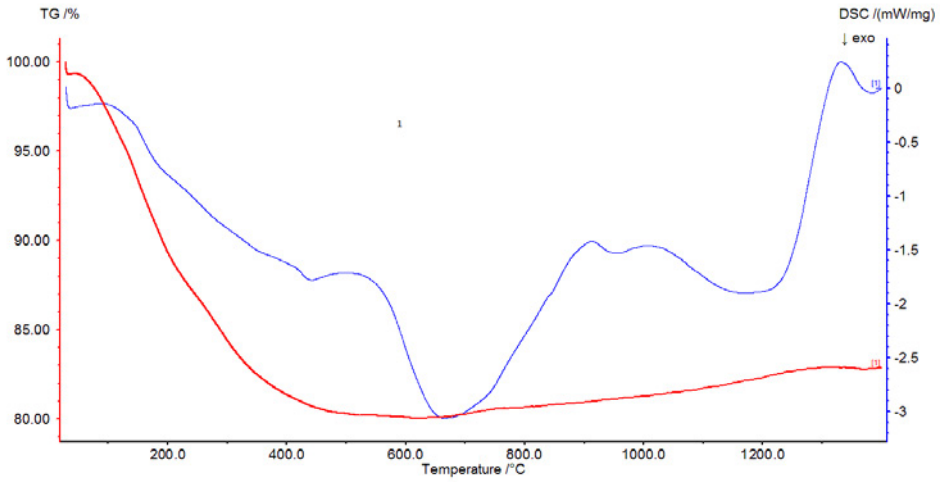

Fig. 5. TGA curves for dried sample.

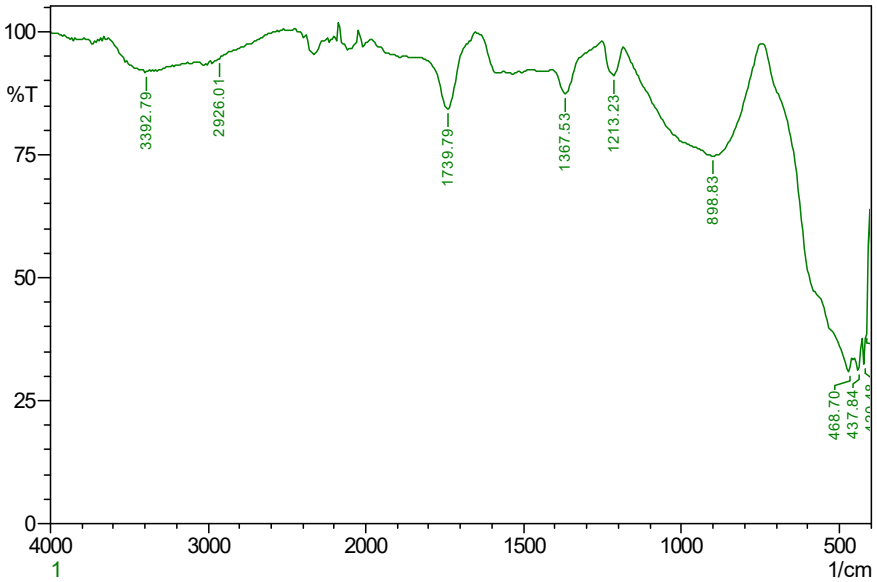

Fig. 6. FTIR spectrum for SnO_2 nanoparticles.

where, Egis the apparent optical band gap, α is an absorption coefficient, h is Planck constant, A is a constant relative to the semiconducting material and 'n' is a value that depends on the nature of transition (n=2 for direct band gap, 2/3 for direct forbidden gap and ½ for indirect band gap). v is the frequency and hv is the incident photon energy. Fig.9 represents the plot of $(\alpha hv)^2$ vs hv for SnO_2 nanocrystallites.

The direct band gap (Eg) of our samples is measured from the absorption coefficient data as a function of wavelength using Tauc relation. By extrapolating the straight line of the $(\alpha hv)^2$ vs hv plot, the energy band gap was found to 3.05 eV. It is clear that obtained tin oxide has the optical band gap larger than the value of 3.64 eV for bulk SnO_2 [13-14].

Photoluminescence Spectra

Photoluminescence (PL) spectroscopy is a suitable technique to determine the crystalline quality and the exaction fine structure. PL measurements at room temperature were performed to know the optical properties of

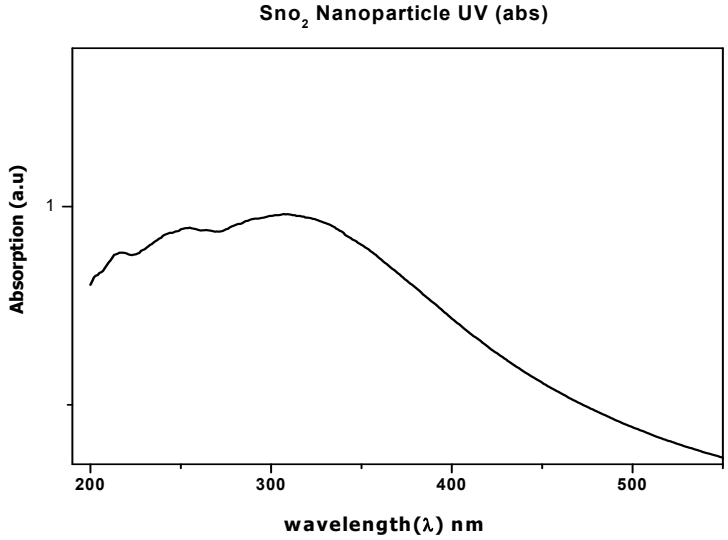

Fig. 7. UV-Vis absorption spectrum of SnO_2 nanoparticles.

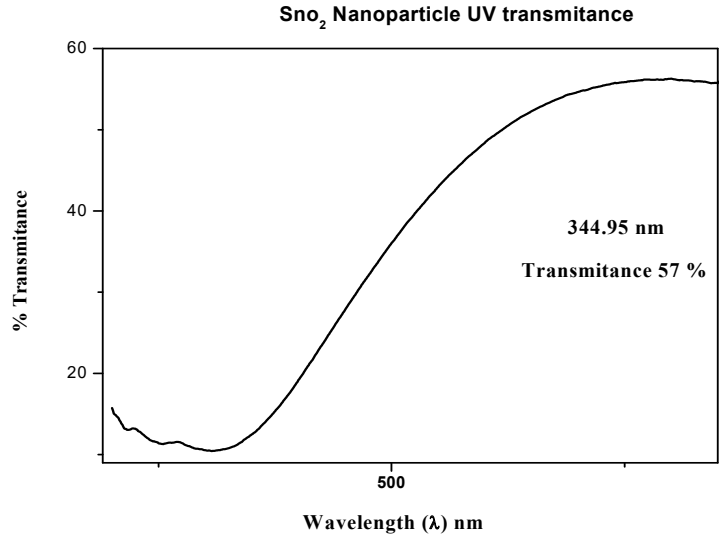

Fig. 8. Transmittance spectrum of SnO_2 nanoparticles.

SnO_2. Fig. 8 represents the PL spectrum of SnO_2 nanoparticles at room temperature. The sample exhibits two strong emission bands at 605 and 651 nm. Since the energy gap of bulk SnO_2 is 3.62 eV the two observed PL bands cannot be assigned to direct recombination of a conduction electron in the Sn, 4d band with a hole in the O, 2p valence band. [15]. Generally, defects such as oxygen vacancies are known to be the most common defects in oxides which are responsible for the broad peaks at higher wavelength and are consistent with the earlier reports[16-19] The sharp band at 567 nm is attributed to oxygen vacancies, which are mainly located on the surface of the nanostructures and can form a series of metastable energy levels within the band gap of SnO_2 by trapping electrons from the valence band to make a contribution to the luminescence or Sn interstitials that have formed during the synthesis process [20].

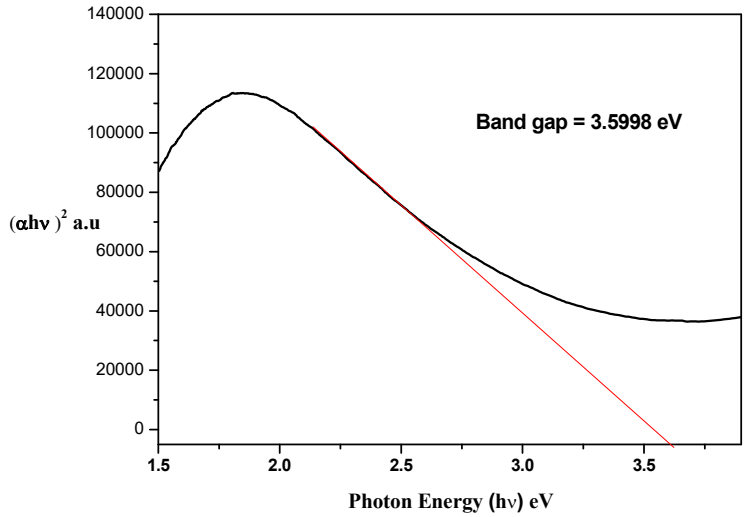

Fig. 9. The plot of (αhν)2 vs hν for SnO_2 nanoparticles.

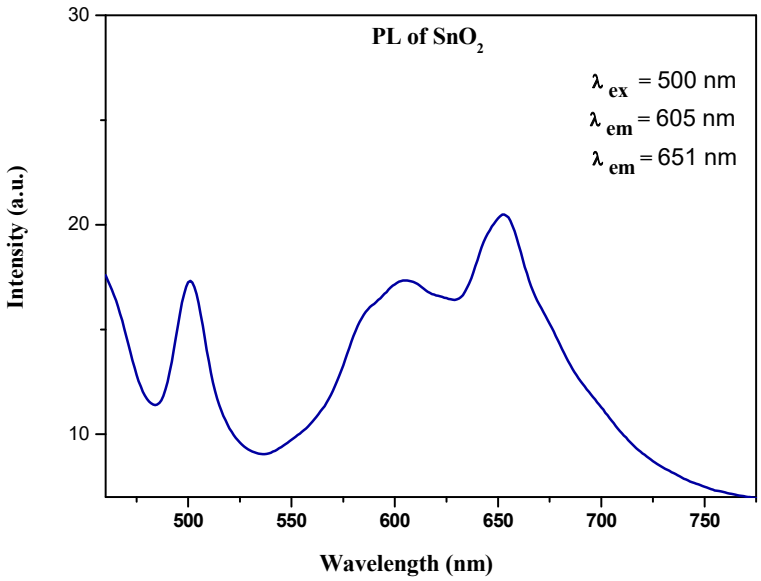

Fig. 10. Photoluminescence spectra of the SnO_2 nano particles.

HR-TEM Analysis

Fig. 9 (a, b) shows the HRTEM micrograph of the synthesized SnO_2 sample. The size of the particles estimated from the HR-TEM image is about 20.52 nm. From Fig.9 clear lattice fringes indicate the established crystallinity of SnO_2 nanoparticles. The distance between the consecutive lattice fringes was found to be 0.39 nm which is in good agreement with the lattice spacing of (110) plane in the SnO_2. Moreover, this is also in agreement with the XRD analytical result, which, in turn, implies that the SnO_2 nanoparticle with small average particle size is well crystallized.

Fig. 9(c) shows the electron diffraction patterns of the sample. It is clear from Fig. 9(c) that the SnO_2 particles are crystalline in nature. The electron diffraction patterns show continuous ring patterns without any additional diffraction spots and rings of secondary phases, revealing their crystalline structure. It has been found that the fringe patterns corresponding to planes (110), (101), (200), (211), (220), (310), and (301) are consistent with the peaks observed in the XRD patterns. XRD and HR-TEM studies confirmed the pure tetragonal structure of SnO_2. For the tetragonal phase of SnO_2, Gu et al reported that the (110) and (001) surfaces have the lowest and the highest surface energies, respectively [6-7].

Hall Effect

Besides the above characteristics, we also determine the Hall coefficient for the prepared

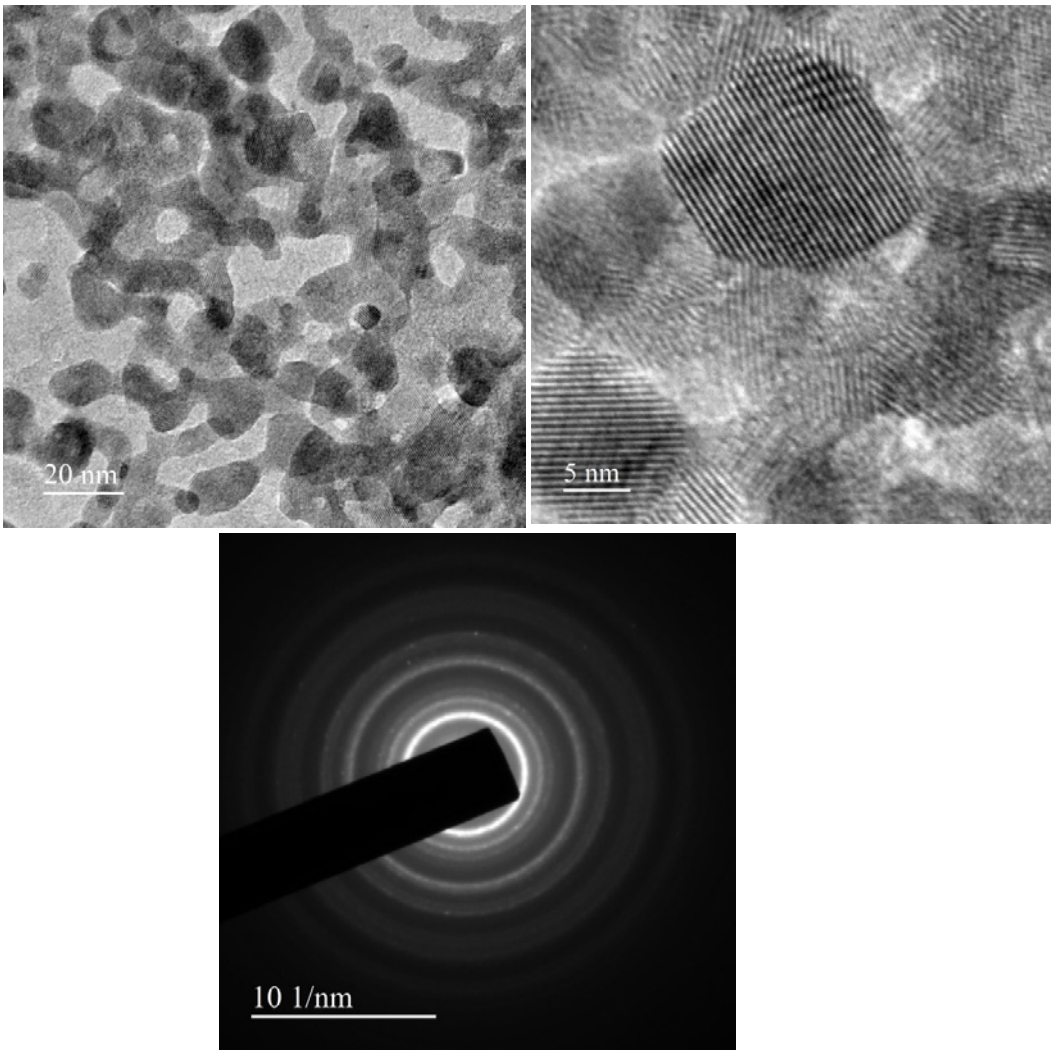

Fig. 11. HR-TEM image and SAED pattern of the SnO_2 sample.

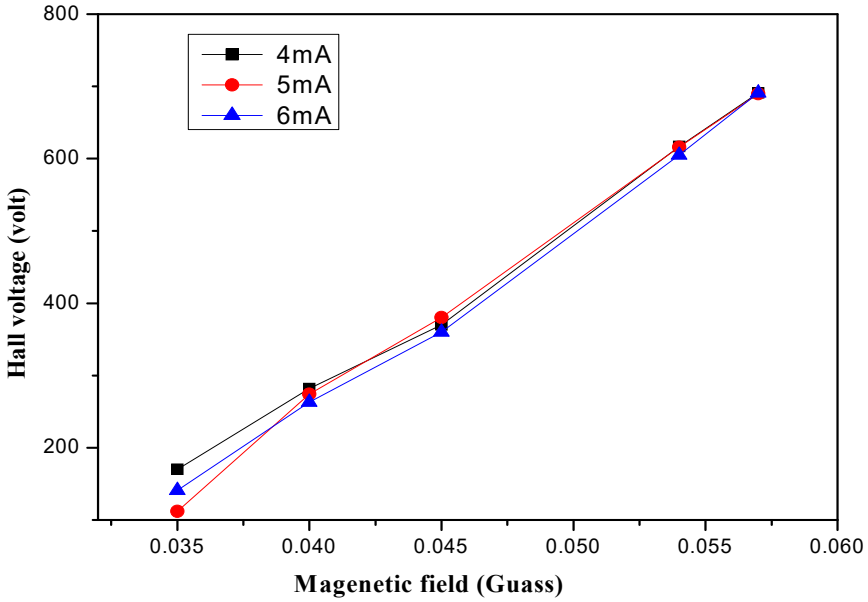

Fig. 12. Hall effect measurement for 4, 5 and 6mA.

sample. It is used to identify the nature of semiconductor. The Hall voltage (V_H) was measured as a function of the perpendicular magnetic field (B) for different drive currents (I). These measurements were performed for different temperatures. The drive current is supplied by Keighley ac current source, which is fed to the reference input of an EG and G instruments of DSP lock-in amplifier, which measures the Hall voltage. The measurements frequency is f = 227Hz.

Hall voltage was measured for various values of applied magnetic field and current through the samples at room temperature as shown in Fig 10. From Fig.10, the Hall voltage (VH) increases with the bias current. From the Hall Effect studies, it is observed that the conductivity and carrier mobility are linearly related while the carrier mobility is inversed of the carrier density. The Hall voltages have been found to be indicating that the n-type semiconductor [21]. The Hall coefficient (R_H) and carrier concentration (n) have been determined.

CONCLUSION

In conclusion, tetragonal shape SnO_2 nanoparticles have been successfully prepared by co-precipitation method. The structural properties of the prepared SnO_2 sample were investigated using the XRD pattern the average crystallite size was found to be 54 nm. Further, thermal and optical properties have also been investigated by TGA, UV-Vis, and PL studies. Here, UV-Vis analysis showed the characteristic absorbance peak at 345 nm. In addition, the band gap of was estimated to be 3.05 eV which is greater than that of the bulk SnO_2. In the PL emission spectrum, three peaks were found at 500, 605 and 651nm, due to the oxygen vacancy defect. Finally, Hall coefficient was also estimated for various values of an applied magnetic field and bias current applied to the sample. From the detailed study, it has been found that the prepared sample is an n-type semiconductor.

CONFLICT OF INTEREST

The authors declare that there are no conflicts of interest regarding the publication of this manuscript.

REFERENCES

1. Park M. S., Kang Y. M., Wang G. X., Dou S. X., Liu H. K., (2008), The effect of morphological modification on the electrochemical properties of SnO_2 nanomaterials. *Adv. Func. Mat.* 18: 455-461.
2. Dawar A. L., Joshi J. C., (1984), Review semiconducting transparent thin films: Their properties and applications. *J. Mater. Sci.* 19: 1-23.
3. Hernandez-Ramirez F., Prades J. D., Tarancon A., Barth S., Casals O., Jiménez-Diaz R., Morante J. R., (2007), Portable microsensors based on individual SnO_2 nanowires. *Nanotechnol.* 18: 495501-495505.
4. Park M. S., Wang G. X., Kang Y. M., Wexler D., Dou S. X., Liu H. K., (2007), Preparation and electrochemical

properties of SnO_2 nanowires for application in lithium-ion batteries. *Ang. Chem. Inter. Ed.* 46: 750-753.
5. Harrison P. G., Bailey C., Azelee W., (1999), Modified Tin (IV) Oxide (M/SnO_2 M= Cr, La, Pr, Nd, Sm, Gd) Catalysts for the oxidation of carbon monoxide and propane. *J. Catal.* 186: 147-159.
6. Agrahari V., Mathpal M. C., Kumar M., Agarwal A., (2015), Investigations of optoelectronic properties in DMS SnO_2 nanoparticles. *J. Alloys & Comp.* 622: 48-53.
7. Gu F., Wang S. F., Lü M. K., Zhou G. J., Xu D., Yuan D. R., (2004), Photoluminescence properties of SnO_2 nanoparticles synthesized by sol–gel method. *J. Phys. Chem. B.* 108: 8119-8123.
8. Gu F., Wang S. F., Song C. F., Lü M. K., Qi Y. X., Zhou G. J., Yuan D. R., (2003), Synthesis and luminescence properties of SnO_2 nanoparticles. *Chem. Phy. Lett.* 372: 451-454.
9. Naje A. N., Norry A. S., Suhail A. M., (2013), Preparation and characterization of SnO_2 nanoparticles. *Int. J. Innov. Res. Sci. Eng. Tech.* 2: 7068-7072.
10. Anandan K., Rajendran V., (2010), Size controlled synthesis of SnO_2 nanoparticles: Facile solvothermal process. *J. Non-Oxide Glasses*. *2*: 83-89.
11. Tan L., Wang L., Wang Y., (2011), Hydrothermal synthesis of SnO_2 nanostructures with different morphologies and their optical properties*. J. Nanomate*r. Article ID 529874, 10 page.
12. Sathyaseelan B., Senthilnathan K., Alagesan T., Jayavel R., Sivakumar K., (2010), A study on structural and optical properties of Mn-and Co-doped SnO_2 nanocrystallites. *Mat. Chem. Phy.* 124: 1046-1050.
13. Aurbach D., Nimberger A., Markovsky B., Levi E., Sominski E., Gedanken A., (2002), Nanoparticles of SnO produced by sonochemistry as anode materials for rechargeable lithium batteries. *Chem. Mater.* 14: 4155-4163.
14. Azam A., Habib S. S., Salah N. A., Ahmed F., (2013), Microwave-assisted synthesis of SnO_2 nanorods for oxygen gas sensing at room temperature. *Int. J. Nanomed. 8*: 3875-3878.
15. Sathyaseelan B., Anand C., Mano A., Zaidi S. M., Jayavel R., Sivakumar K., Vinu A., (2010), Ultrafast microwave assisted synthesis of mesoporous SnO_2 and its characterization. *J. Nanosci. Nanotech.* 10: 8362-8366.
16. Davar F., Salavati-Niasari M., Fereshteh Z., (2010), Synthesis and characterization of SnO_2 nanoparticles by thermal decomposition of new inorganic precursor. *J. Alloys Comp.* 496: 638-643.
17. Aziz M., Abbas S. S., Baharom W. R. W., (2013), Size-controlled synthesis of SnO_2 nanoparticles by sol–gel method. *Mater. Lett.* 91: 31-34
18. Nejati-Moghadam L., Esmaeili Bafghi-Karimabad A., Salavati-Niasari M., Safardoust H., (2015), Synthesis and characterization of SnO_2 nanostructures prepared by a facile precipitation method. *J. Nanostuc.* 5: 47-53.
19. Vyas G., Kumar A., Bhatt M., Bhatt S., Paul P., (2018), New route for synthesis of Fluorescent SnO_2 nanoparticles for selective sensing of Fe(III) in aqueous media. *J. Nanosci. Nanotechnol.* 18: 3954-3959.
20. Elango G., Roopan S. M., (2016), Efficacy of SnO_2 nanoparticles toward photocatalytic degradation of methylene blue dye. *J. Photochem. Photobiol. B: Biology.* 155: 34-38.
21. Faglia G., Baratto C., Sberveglieri G., Zha M., Zappettini A., (2005), Adsorption effects of NO_2 at ppm level on visible photoluminescence response of SnO_2 nanobelts. *App. Phys. Lett.* 86: 011923-011926.
22. Huang L. S., Pu L., Shi Y., Zhang R., Gu B., Du Y., Wright S., (2005), Controlled growth of well-faceted zigzag tin oxide mesostructures. *Appl. Phys. Lett.* 87:163124-163128.